Experimental Research

INTERNATIONAL JOURNAL OF SURGERY

OPEN

Ex vivo lung perfusion with GLP-1R agonist mitigates ischemia/reperfusion injury through pyroptosis modulation in lung transplantation– an experimental study

Yufei Zhang, MD[a], Tao Liu, MD[b,c,d], Huaizu Guo, MD, PhD[b,d], Jianxin Shi, MD[a], Jun Yang, MD[a], Shijie Fu, MD[a], Xufeng Pan, MD[a], Feng Li, MD[e], Hai Zhang, MD[e], Dawei Zhang, PhD[f], Hong Yang, PhD[g,*], Lulu Zheng, PhD[f,*], Meng Shi, MD, PhD[h,*], Wenyong Zhou, MD, PhD[a,*]

Background: Ischemia/reperfusion injury (IRI) presents a significant hurdle in lung transplantation. Our previous research showed that the glucagon-like peptide-1 receptor (GLP-1R) agonist liraglutide (Lir) improves lipopolysaccharide-induced acute lung injury in murine models. This study aims to further investigate the lung-protective mechanisms of GLP-1R agonist.

Methods: An in vitro hypoxia/reoxygenation (H/R) model with BEAS-2B cells and an in vivo donation after cardiac death (DCD) rat lung transplant model were utilized. Lir was administered using an ex vivo lung perfusion (EVLP) system. Lung function, injury, and pyroptosis mechanisms were assessed. Validation experiments included quantitative reverse transcription PCR, immunoblot analysis, activity assays and proteomic analysis, among others, to evaluate how GLP-1R agonist protect lungs from IRI by modulating pyroptosis, thereby improving lung function and reducing injury.

Results: Perfusion of the donor lung with Lir using EVLP improved the function of DCD lungs and mitigated IRI. Bioinformatics analysis and validation experiments provided evidence of increased expression of NOD-like receptors signals and pyroptosis in lung transplantation IRI, which was suppressed by Lir treatment. Further investigations revealed that the thioredoxin-binding protein (TXNIP) played a crucial regulatory role in the pyroptosis of IRI, with the NOD-like receptor family pyrin domain-containing 3 (NLRP3) emerging as a key target. In addition, this study found that Lir promotes GLP-1R-dependent TXNIP ubiquitination and modulates TXNIP mRNA stability via the GLP-1R/miR-17 axis.

Conclusion: This study demonstrates, for the first time, that a novel EVLP-based drug delivery approach using GLP-1R agonist can protect lungs from IRI by modulating pyroptosis, thereby improving lung function and reducing injury. The research uncovers a previously unknown mechanism where GLP-1R agonist modulates the protein TXNIP through GLP-1R/miR-17 signaling. These insights underscore the potential of GLP-1R agonists as targeted therapies for primary graft dysfunction in lung transplant recipients, opening new avenues for clinical interventions to improve transplant outcomes.

Keywords: ex vivo lung perfusion (EVLP), GLP-1R agonist, ischemia/reperfusion injury (IRI), pyroptosis, thioredoxin-binding protein (TXNIP)

Introduction

Ischemia/reperfusion injury (IRI) is the primary etiology of primary graft dysfunction (PGD) after lung transplantation[1]. Concurrently, lung transplant IRI serves as a significant risk factor for exacerbating infections and transplant rejection, leading to graft dysfunction and lung transplant failure[2,3]. Given that donor lungs undergo essential procedures, including cold preservation and transplant reperfusion, eliminating pathogenic triggers becomes challenging in mitigating lung transplant IRI. Consequently, inhibiting or ameliorating lung transplant IRI progression offers a potential avenue for addressing this issue.

[a]Department of Thoracic Surgery, Shanghai Chest Hospital, Shanghai Jiao Tong University School of Medicine, Shanghai, China, [b]State Key Laboratory of Macromolecular Drugs and Large-scale Preparation, School of Pharmaceutical Sciences, Wenzhou Medical University, Wenzhou, China, [c]Department of Oncology, Huashan Hospital, Fudan University, Shanghai, China, [d]State Key Laboratory of Macromolecular Drugs and Large-scale Preparation, School of Pharmaceutical Sciences and Food Engineering, Liaocheng University, Liaocheng, China, [e]Department of Pulmonary Medicine, Shanghai Chest Hospital, Shanghai Jiao Tong University School of Medicine, Shanghai, China, [f]Engineering Research Center of Optical Instrument and System, The Ministry of Education, Shanghai Key Laboratory of Modern Optical System, University of Shanghai for Science and Technology, Shanghai, China, [g]The Province and Ministry Co-Sponsored Collaborative Innovation Center for Medical Epigenetics, Department of Pharmacology and Tianjin Key Laboratory of Inflammation Biology, School of Basic Medical Sciences, Tianjin Medical University, Tianjin, China and [h]Department of Thoracic and Cardiovascular Surgery, Huashan Hospital, Fudan University, Shanghai, China

Yufei Zhang, Tao Liu, Huaizu Guo, and Jianxin Shi contributed equally to this work.

*Corresponding author. Address: Mailing address: No 421, Huaihai West Road, Shanghai 200030, China. Tel.: +86-15821673400;
E-mail: zhou.wenyong@shsmu.edu.cn (W. Zhou); mengshi@fudan.edu.cn (M. Shi); llzheng@usst.edu.cn (L. Zheng); hongyang@tmu.edu.cn (H. Yang).

International Journal of Surgery (2025) 111:3781–3797

Received 25 November 2024; Accepted 14 April 2025

Supplemental Digital Content is available for this article. Direct URL citations are provided in the HTML and PDF versions of this article on the journal's website, www.lww.com/annals-of-medicine-and-surgery.

Published online 16 May 2025

http://dx.doi.org/10.1097/JS9.0000000000002438

Glucagon-like peptide-1 (GLP-1), a polypeptide hormone primarily secreted by the intestinal L cells and pancreatic α cells, plays a significant role in the physiological regulation across various organs through the activation of GLP-1 receptors (GLP-1Rs)[4]. Our previous research has demonstrated that the GLP-1R agonist (GLP-1RA) liraglutide (Lir) can significantly alleviate lipopolysaccharide (LPS)-induced acute lung injury in mice models[5]. Additionally, GLP-1RAs have been shown to effectively modulate oxidative stress[6,7], suggesting their potential utility in improving lung transplant outcomes involving IRI. This study aimed to explore the efficacy and underlying mechanisms of GLP-1RA in mitigating IRI in lung transplantation, specifically focusing on organs donated after cardiac death (DCD)[8].

In contrast to the traditional method of immediate transplantation following donor lung procurement, leading lung transplant centers are increasingly adopting the ex vivo lung perfusion (EVLP) system. This sophisticated system not only evaluates the viability of marginal donor lungs prior to transplantation[9] but is also acclaimed for its therapeutic potential in repairing and reconditioning donor lungs, extending beyond its initial evaluative purpose[9-12]. Strategically positioned between the phases of cold preservation and transplant reperfusion, EVLP provides a critical interval in the IRI process, offering a valuable opportunity for the prevention or intervention of IRI[9]. In this study, EVLP is innovatively utilized as a delivery platform for Lir and as a tool for the real-time assessment of donor lung quality.

IRI is recognized for inducing cellular death, thereby perpetuating a deleterious cycle that exacerbates tissue damage[13]. Recent studies have identified a significant association between the apoptosis of type II alveolar epithelial cells and IRI within the context of lung transplantation[1,2,14]. As the duration of ischemia increases, necrosis supersedes apoptosis as the predominant form of cell death[13]. The potential role of GLP-1RA in mitigating cellular death, particularly inflammatory cell death during lung transplantation, remains a promising area for further investigation.

Pyroptosis is a process in which NLR family members (NLRP3, AIM2, NLRP1, NLRC4) serve as cytoplasmic pattern recognition receptors (PRR) to recognize intracellular trigger signals such as reactive oxygen species (ROS). This detection triggers the activation of Gasdermin D via inflammasome-mediated pathways, ultimately resulting in the release of interleukin-1β (IL-1β) and interleukin-18 (IL-18)[15,16]. The activation of inflammasomes is a pivotal event in the process of pyroptosis[15]. Inflammasome activation varies among different types, with AIM2, NLRP1, and NLRC4 primarily associated with specific bacterial or viral infections. In contrast, the activation of the NOD-like receptor family pyrin domain-containing 3 (NLRP3) is generally triggered by exposure to pathogen-associated molecular patterns (PAMPs) or damage-associated molecular patterns (DAMPs)[15,17]. Pyroptosis is a distinct form of cell death, differing from apoptosis and necrosis, due to its capacity to induce significant tissue inflammation, highlighting its unique influence on tissue pathology. Although traditionally observed in innate immune cell such as macrophages, dendritic cells (DC), and natural killer (NK) cells[15], pyroptosis has also been noted in non-immune cells within donor lungs following leukocyte removal during EVLP[18]. This observation suggests a potential role for pyroptosis in non-immune cells during IRI in lung transplantation. Consequently, a thorough understanding of the intracellular signaling pathways that trigger inflammasome activation and subsequent induce pyroptosis is crucial. Such understanding could offer valuable insights into mitigating IRI in lung transplantation, underscoring the importance of targeting pyroptosis as a potential therapeutic strategy in this context.

HIGHLIGHTS

- Perfusion of the donor lung with Lir using EVLP improved the function of DCD lungs and mitigated IRI.
- The expression of NOD-like receptors signals and pyroptosis were increased in lung transplantation IRI, which was suppressed by Lir treatment.
- The thioredoxin-binding protein (TXNIP) played a crucial regulatory role in the pyroptosis of IRI, with the NOD-like receptor family pyrin domain-containing 3 (NLRP3) emerging as a key target.
- Lir promotes GLP-1R-dependent TXNIP ubiquitination and modulates TXNIP mRNA stability via the GLP-1R/miR-17 axis.
- These insights underscore the potential of GLP-1R agonists as targeted therapies for primary graft dysfunction in lung transplant recipients, opening new avenues for clinical interventions to improve transplant outcomes.

Recent reports have indicated that the thioredoxin-binding protein (TXNIP) plays a critical role for the activation of NLRP3 inflammasomes and the subsequent induction of pyroptosis through its direct interaction with NLRP3[19]. This interaction results in the suppression of both the expression and activity of the redox-regulatory protein thioredoxin (TRX)[20]. Furthermore, increased oxidative stress has been shown to upregulate TXNIP expression and facilitate its translocation to the mitochondria, leading to an accumulation of mitochondrial ROS[21]. Conse quently, TXNIP demonstrates oxidative activities. Nevertheless, the precise roles of ROS and TXNIP in the context of pyroptosis during IRI in lung transplants require further investigation.

Through the integration of bioinformatics analysis of proteomics data, we postulated that IRI in lung transplants induces pyroptosis in non-innate immune cells, a process potentially attenuated by Liraglutide (Lir).

The primary aim of this study is to evaluate the potential protective effects of Lir in the context of lung transplant IRI, specifically through the inhibition of pyroptosis, with a particular emphasis on the involvement of TXNIP. This study expands on previous findings by demonstrating the protective effects of liraglutide, against IRI in a robust experimental setup involving both cell culture and a donation after DCD rat lung transplantation model. Notably, the innovative application of EVLP for liraglutide administration offers a novel therapeutic strategy that could enhance lung function and minimize injury during transplantation. This research has the potential to inform the development of innovative therapeutic strategies aimed at improving lung transplantation outcomes by targeting pyroptotic pathways. Overall, this work not only strengthens the case for liraglutide as a viable agent in preventing IRI but also paves the way for further investigations into EVLP-based drug delivery systems in lung transplantation. The findings hold significant promise for improving transplant outcomes and patient recovery, suggesting that preconditioning donor lungs with protective agents could become a standard practice in the field.

Materials and methods

Animals

Adult Sprague-Dawley rats (10–12 weeks, 360–400 g) were used in all the experiments. All animals received humane care in compliance with the "Guide for the Care and Use of Laboratory Animals" (NIH Publication No. 86-23, revised 1996). The work has been reported in accordance with the ARRIVE guidelines (Animals in Research: Reporting In Vivo Experiments)[22]. The study was approved by the Ethics Committee. In the ethical approval document, the experimental design, research grouping plan, experimental methods employed, the number of experimental animals used, and the principles of animal welfare are all described in detail.

Donor lungs preparation and experimental design

As previously detailed[23], anesthesia of donor rats was induced with inhaled isoflurane (5%) and maintained with ketamine (80 mg/kg) and xylazine (8 mg/kg) intraperitoneally. Animals were placed on heating plates to maintain a body temperature of 37°C, tracheotomized, and mechanically ventilated (fraction of inspired oxygen (FiO_2) 0.21, tidal volume (Vt) 8 mL/kg). Following a median sternotomy, heparin (1000 U) was injected into the right ventricle. The pulmonary artery (PA) and left atrium (LA) were cannulated.

The donor rats were sacrificed by exsanguination and allocated to one of the following groups (Figure S1A, http://links.lww.com/JS9/E136). Cold ischemia transplantation group (CI LTx): Lungs were flushed through the PA cannula with 15 mL of 4°C Perfadex (Xvivo Perfusion, Göteborg, Sweden). The heart-lung block was then removed, and the lungs were preserved in an inflated status (FiO_2 = 0.5) for 5 hours in 4°C Perfadex (CI). Warm ischemia transplantation group (WI LTx): Lungs were kept in situ for 60 minutes of "no-touch" warm ischemia (WI), then flushed with 15 mL of 4°C Perfadex. The heart-lung was preserved in an inflated status (FiO_2 = 0.5) for 4 hours in 4°C Perfadex. EVLP transplantation group (EVLP LTx): Lungs were kept in situ for a 60-minute period of warm ischemia, then flushed with 15 mL of 4°C Perfadex. The heart-lung block was preserved in an inflated status (FiO_2 = 0.5) for 1 hour in 4°C Perfadex. Then, the heart-lung blocks were subjected to EVLP for 3 hours. EVLP + Lir transplantation group (EVLP + Lir LTx): Same as EVLP LTx group, except that Lir (Novo Nordisk, Bagsværd, Denmark) was added in EVLP system at a concentration of 100 nM. After completing the corresponding procedures, the donor lungs of the four groups were used for test samples or prepared for pulmonary vascular cuffing on 4°C moist gauze, and then orthotopic lung transplantation was performed using the left single lung. Sham group: After anesthesia and mechanical ventilation, the rats underwent thoracotomy only. After 7.5 hours of chest closure, the rats were sacrificed to obtain lung tissue for the subsequent experiment.

EVLP

A diagram of the murine EVLP system is shown in FigureS1B. http://links.lww.com/JS9/E136. The EVLP system for rats (IL-2; Hugo Sachs Elektronik, March, Germany) was previously described[23]. The heart-lung blocks were mounted and perfused at progressive flow (2% of the rat cardiac output at 10°C, up to 7.5% of cardiac output at 37.5°C) with Steen solution (Xvivo Perfusion) equilibrated with 6% O_2, 10% CO_2, and 84% N_2. For the EVLP + Lir group, Lir (100 nM) was added to Steen solution. The ventilation started at 35°C (RR: 7/min, Vt: 3 mL/kg, positive end-expiratory pressure (PEEP): 3 cm H_2O, FiO_2: 0.21). At 37°C, Vt was set at 6 mL/kg. The EVLP sensor collected pulmonary artery pressure (PAP), and pulmonary vascular resistance (PVR) data. Pulmonary compliance (PC) was determined by the predefined algorithm. A blood gas analyzer tested the biochemical variables of perfusate during EVLP. At the end of EVLP, the heart-lung blocks were inflated (FiO_2: 0.21) in cold Perfadex (4°C) for further left lung transplant preparation.

Orthotopic left lung transplantation and evaluation of lung graft function

We followed the orthotopic rat lung transplant procedure as described in previous research[24]. Briefly, after using an aneurysm clip to block the left hilum of the recipient rats, 7-0 nylon sutures were placed around the PA, PV, and bronchus for future securing of the cuffs. After making the incision on the PA, PV, and bronchus of the recipient, the cuffed PA, PV, and bronchus of donor lungs were inserted into the corresponding structures of the recipients through an incision. The clip was removed after being secured with 7-0 nylon suture. Lung reperfusion occurs as the recipient's blood flows into the transplanted lung through the anastomosed pulmonary artery. The transplanted lungs are then repositioned in the recipient's thoracic cavity following the full transplant procedure. After 2 hours, the recipient rats were used for further analysis.

To evaluate the lung graft function, anesthetized recipient rats underwent mechanical ventilation of 100% FiO_2 for 3 minutes. Subsequently, the hilum of the native lung was occluded using vascular clamps. After 3 minutes of ventilation, arterial blood was withdrawn from the left ventricle using a 1 mL heparin-coated syringe for arterial blood gas measurement.

Lung wet/dry weight ratio

The fresh lung graft was weighed first, followed by a drying procedure in an oven at 80 °C for 48 hours, and lung weight were measured again.

Protein concentration and cell count in bronchoalveolar lavage fluid

After an intratracheal injection of 800 μL of phosphate-buffered saline (PBS) into the lung graft, bronchoalveolar lavage fluid (BALF) was collected. The BALF was centrifuged at 400 G for 5 minutes at 4 °C. The cell-free BALF supernatant was processed using a bicinchoninic acid (BCA) protein assay kit to measure the protein concentration. The pelleted cells were resuspended and counted with a hemocytometer.

Lung injury scoring

For the histological study, lung grafts were fixed in 4% paraformaldehyde overnight, embedded in paraffin, and sectioned for hematoxylin and eosin (H&E) staining. The grading of the lung pathology was performed by the pathologist in a blinded fashion, using standard criteria. Pathological categories included neutrophils in alveolar spaces, neutrophils in interstitial spaces, hyaline membrane formation, proteinaceous debris in airspaces,

and alveolar septal thickening. Each category was scored on a 0-4 scale (0: absent, 1: mild, 2: moderate, 3: severe, 4: very severe). Total scores were averaged across five fields per sample. Scoring was performed by a pathologist in a blinded fashion using established criteria, as described in our prior work[25,26].

Quantitative real-time polymerase chain reaction

Gene expression was quantified by quantitative real-time polymerase chain reaction (qRT-PCR) by an ABI Prism 7900 Sequence Detection System (Applied Biosystems, Waltham, MA, USA). The data were normalized relative to the expression of β-actin.

Immunoblot analysis

Briefly, protein lysates from the lung grafts or cell cultures were subjected to sodium dodecyl sulfate-polyacrylamide gel electrophoresis (SDS-PAGE) and then transferred to nitrocellulose membranes. The membranes were incubated with anti-TXNIP (1:1000; Cell Signaling Technology (CST), Danvers, MA, USA), anti-NLRP3 (1:1000; CST), anti-GLP-1R (1:500; Santa Cruz Biotechnology, Santa Cruz, CA, USA) or anti-GAPDH (1:1000; Sigma-Aldrich, Waltham, MA, USA) overnight at 4 °C. The horseradish peroxidase (HRP)-labeled secondary antibody (1:2000: CST) was added and incubated for 1 hour at room temperature. Protein bands were detected by the enhanced chemiluminescence (ECL) western blotting (WB) detection system.

Immunohistochemistry staining

For GLP-1R detection in mouse pancreatic islets and lungs, a monoclonal antibody (Mab 7F38) described by Jensen *et al* was used[27] The immunohistochemistry (IHC) staining for cleaved-Caspase-1 and cleaved-Caspase-3 in lung grafts was performed as described previously[5].

Flow cytometry analysis

The cell death in cell cultures was detected by flow cytometry through Annexin V and propidium iodide (PI) staining as described previously[28]. Flow cytometry data were collected on a FACSCaliber instrument (Becton, Dickinson and Company (BD) Biosciences, Franklin Lakes, NJ, USA) and analyzed by the FlowJo software (Tree Star, Ashland, OR, USA).

Enzyme-linked immunosorbent assay detection

We detected levels of cytokines IL-6, TNF-α, IL-1β, IL-18, IL-10, and chemokine CXCL2 in the EVLP perfusate of donor lungs by using the enzyme-linked immunosorbent assay (ELISA) detection kit (BD Biosciences; Thermo Fisher Scientific) according to the manufacturer's protocol. The concentration of IL-1β, IL-18, and TXNIP was also detected in the supernatant of cell culture and BALF, or cell lysates of BALF.

ROS detection

The ROS levels were measured in lung grafts and cell cultures by commercially available assay (Invitrogen, Carlsbad, CA, USA). According to the manufacturer's recommendation, we resuspended the lung graft homogenate and cell culture in the assay buffer. A microplate reader detected the cell-permeable fluorogenic probe to evaluate the ROS levels.

Quantification of superoxide production

The superoxide content in lung grafts and cell cultures was determined by lucigenin-enhanced chemiluminescence as previously described[29]. A luminometer measured the lucigenin-enhanced chemiluminescence.

TRX activity

TXNIP binds and negatively modulates the activity of TRX. The TXNIP activity can be measured by TRX activity. We used the insulin disulfide reduction assay in tissue homogenates and cell lysate to detect TRX activity as previously described[30].

Lactate dehydrogenase activity

According to the manufacturer's recommendation, we measured cell death in lung grafts and cell cultures by a lactate dehydrogenase (LDH) assay kit (Abcam, Cambridge, MA, USA).

Caspase-1 and Caspase-3 activity

We detected the activity of Caspase-1 and Caspase-3 in cell cultures by using the Caspase-1 and Caspase-3 activity assay kit (Beyotime, Shanghai, China) according to the manufacturer's recommendation.

Proteomic analysis

We subjected three lung graft samples from the EVLP LTx group and three lung graft samples from the EVLP + Lir LTx group to TMT-based proteomic analysis. After protein extraction and digestion, TMT labeling of peptides, and mass spectrometry analysis as described previously[31]. The raw data were imported into proteome discoverer software (version 2.4; Thermo Fisher Scientific). Differentially expressed proteins (DEPs) were screened with the cut-off of a ratio fold-change of >1.20 and *P*-values <0.05. We explored the mechanism for biological changes by bioinformatics analysis. Gene Ontology (GO) enrichment and the Kyoto Encyclopedia of Genes and Genomes (KEGG) were adopted.

Hypoxia/reoxygenation-induced BEAS-2B cells (include MnTMPyP, Actinomycin D, and MG132 pretreatment)

Human lung epithelial BEAS-2B cells were cultured in Dulbecco's modified Eagle medium (DMEM) containing 10% fetal bovine serum (FBS) at 37 °C in 5% CO_2 and 95% O_2, and pretreated with control agent, MnTMPyP, or Actinomycin D alone. To establish the hypoxia/reoxygenation (H/R) model, cell culture were placed in sealed boxes, and the sealed containers were purged of gas using 95% N_2 and 5% CO_2 for 25 minutes. Then, the cells were kept in a hypoxic environment at 37°C for 3 hours. After hypoxia stimulation, the cells were placed in a 37°C, 95% O_2, and 5% CO_2 cell incubator for 1 hour to complete the cell H/R induction.

MTS assay for BEAS-2B cell viability test

Cell viability was measured using a cell proliferation assay (Promega, Madison, WI, USA). BEAS-2B cells were seeded in 96 well plates at a density of 4000 cells/well and subjected to hypoxia at serial times (0 h, 1 h, 3 h, and 6 h), and then assayed. Next, we used H/R-induced BEAS-2B cells to validate the effect of Lir on cell

viability. BEAS-2B cells were treated with Lir (0 nM, 20 nM, 100 nM, or 250 nM) 24 hours before and during the H/R induction.

Recombinant adeno-associated virus infection in animals

We used the recombinant adeno-associated viruses (rAAV) of rAAV5-shTXNIP and rAAV5-TXNIP infection to knock down or overexpress TXNIP in donor lungs for EVLP and following transplantation. The rAAV5s were injected into the bronchus of the donor rats (3×10^{10} PFU, 300 μL) via tracheal intubation[32]. Then, 4 weeks later, the donor lungs of the infected rats were used to establish the DCD transplantation models.

The recombinant adenovirus infection in BEAS-2B cells

We used the recombinant adenovirus (rAd) of rAd-NLRP3 and rAd-shTXNIP infection to overexpress NLRP3 or knock down TXNIP in BEAS-2B cells[33]. After 72 hours of rAd infection, the infection efficiency of each cell group was assessed by western blotting. Further, the rAd-infected BEAS-2B cells were used for H/R induction.

Cell transfection

After being planted for 24 hours, according to the manufacturer's protocol, BEAS-2B cells were transfected with shRNA for 6 hours using Lipofectamine 2000 (Invitrogen, (Invitrogen, Carlsbad, CA, USA). shRNAs directed against miR-17 or GLP-1R was inserted into the pLKO.1 vector. After transfection, the cells were cultured for another 48 hours, and the knockout efficiency was detected by qPCR. miR-17 overexpression in BEAS-2B was achieved by transfection with pcDNA3.1 using Lipofectamine 2000, and the transfection efficiency was illustrated by observing red fluorescent protein under fluorescence microscopy.

Co-immunoprecipitation

For the Co-IP assay, whole-cell lysates were prepared. Target proteins (HA, and MYC) were immunoprecipitated by incubating 800 μg of the extracted proteins with anti-HA or anti- MYC antibody, respectively, at 4°C with rotation overnight. Protein A/G Sepharose (Share-bio, Shanghai, China) was then added and incubated for 2 h on a spinning wheel at 4°C. Subsequently, the beads–antibody complex and protein lysate were suspended. The beads were collected by centrifugation at 3000 g, followed by three washes with lysis buffer. Following this, the immunoprecipitates were analyzed using western blot. Secondary antibodies such as anti-rabbit IgG light chain (1:10 000), anti-rabbit IgG heavy chain (1:2000), and anti-mouse IgG light chain (1:5000) were used.

Results

Warm ischemia aggravates IRI in lung transplantation

In order to select a suitable rodent lung transplant model (LTx) with the desired degree of IRI, we utilized warm ischemia (WI) lungs and cold ischemic (CI) lungs for lung transplantation[23], respectively (Figure S1A. http://links.lww.com/JS9/E136). The establishment of DCD models was employed to simulate warm ischemia in the donor lungs. Our findings revealed that two hours post-transplantation, the oxygenation index in recipients WI LTx was significantly lower compared to recipients of CI LTx (Figure S2A. http://links.lww.com/JS9/E136).

Pathological assessment and lung injury scoring are crucial for grading IRI in lung transplantation. The lung grafts in the WI LTx group exhibited severe interstitial and intra-alveolar edema, interalveolar septal thickening, and collapse of pulmonary alveoli. In contrast, CI LTx significantly mitigated the pathological lesions induced by warm ischemia, as evidenced by statistically significant differences in pathology scores. The lung injury score in the WI LTx group was 1.5 times higher than that in the CI LTx group (Figure S2B. http://links.lww.com/JS9/E136). Furthermore, we observed an increase in other indicators that reflect lung transplant IRI, such as the number of nucleated cells and total protein content in bronchoalveolar lavage fluid (BALF), as well as the wet/dry (W/D) ratio in lung grafts (Figure S2C, D, E. http://links.lww.com/JS9/E136). These results indicated that warm ischemia is associated with more severe IRI in lung transplantation. Therefore, WI LTx was chosen for subsequent studies.

EVLP process does not aggravate lung transplant IRI

We aimed to determine whether EVLP exacerbates IRI in lung transplantation. To investigate this, a DCD lung underwent a 3 hours EVLP process (EVLP LTx) prior to transplantation (Figure S1A-C. http://links.lww.com/JS9/E136). Compared to the WI group, the EVLP LTx group exhibited no significant differences in oxygenation index, W/D ratio, mononuclear cells count in BALF, total protein content of BALF, and lung injury score (Figure S2A-E. http://links.lww.com/JS9/E136). These findings suggest that EVLP is an effective method for preserving and potentially repairing lung grafts, without exacerbating IRI in the context of DCD lung transplantation.

Lir suppresses cell death in H/R-induced BEAS-2B cells

In the in vitro study, we used H/R to induce cell dysfunction, simulating IRI in the context of organ transplantation[34,35]. Specifically, we established an H/R model employing human lung epithelial BEAS-2B cells (Figure S3A. http://links.lww.com/JS9/E136) and assessed the impact of hypoxia on cell viability. Notably, significant differences were observed among prolonged hypoxia (6 and 3 hours), short-term hypoxia (1 hours), and the control group (Figure S3B. http://links.lww.com/JS9/E136). To investigate the potential influence of Lir on IRI in lung transplantation, we treated H/R-induced BEAS-2B cells with Lir (0 nM, 20 nM, 100 nM, or 250 nM) for 24 hours. Cell viability exhibited a dose-dependent increase following treatment with Lir (Figure S3C. http://links.lww.com/JS9/E136). Based on these experimental findings, we determined that a 3-hour hypoxic exposure followed by reoxygenation for 1 hour, along with a Lir concentration of 100 nM, would be appropriate conditions for subsequent experiments. The elevation of oxidative stress is an crucial pathological characteristic of IRI in lung transplantation. Notably, treatment with Lir effectively suppressed the up-regulation of ROS and superoxide in H/R-induced BEAS-2B cells (Figure S3D, E. http://links.lww.com/JS9/E136).

Additionally, we assessed the potential impact of Lir on BEAS-2B cells under H/R conditions in an in vitro setting. Our findings revealed a significant increase in both cell death and LDH activity in H/R-induced BEAS-2B cells compared to those cultured under normal conditions (Figure S3F, G. http://links.

lww.com/JS9/E136). However, treatment with Lir markedly decreased both cell death and LDH activity in H/R-induced BEAS-2B cells. These results collectively underscore Lir's protective role against cell death and oxidative stress in H/R-induced BEAS-2B cells, suggesting its potential therapeutic utility in managing IRI during lung transplantation.

Lir improves DCD lung function and repairs injury during EVLP

GLP-1 plays a physiological role in the regulation of the pancreas and other extrapancreatic organs, primarily through its interaction with the GLP-1R[4]. It has been observed that GLP-1R is widely distributed in human lung cells[36]. To further investigate this, we compared GLP-1R-immunostained sections of pancreatic and lung tissues in wild-type C57/B6 mice and GLP-1R$^{-/-}$C57BL/6 mice (provided by Prof. Jin, Toronto General Hospital Research Institute) (Fig. 1A). This comparison revealed a high expression of GLP-1R in rodent lungs, prompting further exploration of the GLP-1RA, Liraglutide, for the treatment of lung injury.

The initial set of analyses investigated the impact of Lir (100 nM) through EVLP perfusion (EVLP + Lir group) (Figure S1A-C. http://links.lww.com/JS9/E136) on pulmonary function. The data obtained from EVLP sensors indicated that, compared to EVLP perfusion alone (EVLP group), the EVLP + Lir group exhibited a significant increase in pulmonary compliance (from 90 to 180 minutes) and reductions in pulmonary artery pressure (PAP) (from 120 to 180 minutes), pulmonary vascular resistance (PVR) (from 90 to 180 minutes), and pulmonary edema (weight gain) (Fig. 1B). Functionally, the EVLP + Lir group demonstrated a higher oxygenation index and a more controlled increase in lactate levels—indicative of reduced cellular hypoxia—compared to the EVLP group from 60 minutes until the end of the EVLP process (Fig. 1C). Additionally, The EVLP + Lir group maintained a higher pH level, while glucose levels remained consistent across both groups (Fig. 1C). The inflammatory response, assessed through the presence of proinflammatory cytokines and chemokines in the EVLP perfusate, showed a significant decrease in IL-6, TNF-α, IL-1β, IL-18, and CXCL2 levels in the EVLP + Lir group compared to the EVLP group, whereas IL-10 levels increased (Fig. 1D), suggesting an anti-inflammatory effect of Lir treatment. To further evaluate the protective effects of Lir on lung injury, a histopathological examination was conducted. Consistent with the observed changes in lung function, the application of H&E staining and histological scoring revealed a reduction in injury following Lir perfusion (Fig. 1E). The lung tissue of the control group exhibited severe degrees of inflammatory cell infiltration, interstitial and intra-alveolar edema, and patchy hemorrhage, interalveolar septal thickening, and hyaline membrane formation, with associated collapsed pulmonary alveoli. These findings suggest that Lir treatment via EVLP improves lung function in DCD cases and facilitates the repair of lung injuries.

Lir perfusion by EVLP against IRI in lung transplantation

While the protective effects of Lir on H/R-induced BEAS-2B cells and DCD lungs have been established, it remains unclear whether Lir mitigates IRI during lung transplantation. To investigate the role of Lir perfusion through EVLP in lung transplant IRI, DCD lungs were subjected to either EVLP or EVLP plus Lir perfusion before lung transplantation. Initially, the oxygenation index was assessed in recipients who received either EVLP or EVLP plus Lir-perfused donor lungs. Compared to the EVLP group, the findings indicated a significant increase in the oxygenation index among recipients of the EVLP + Lir group (Fig. 2A).

Pathological assessments demonstrated that the EVLP + Lir-treated lung grafts exhibited notable reductions in inflammation and edema compared to the EVLP group (Fig. 2B). Blinded pathological scoring quantitatively supported this observation, revealing significantly lower lung injury scores in the EVLP + Lir group (Fig. 2B). Moreover, Lir perfusion markedly decreased mRNA levels of pro-inflammatory cytokines (IL-6, TNF-α, IL-1β, and IL-18) and the chemokine (CXCL2) in lung grafts (Fig. 2C), illustrating its anti-inflammatory effects.

As previously mentioned, the administration of Lir treatment effectively mitigated oxidative stress in BEAS-2B cells under H/R conditions. This finding was further corroborated by the notable reduction in the levels of ROS and superoxide observed in lung grafts following Lir perfusion (Fig. 2D). In terms of cell death, our findings indicate a significant decrease in the presence of cleaved Caspase-3-positive cells and LDH activity in lung grafts of the EVLP + Lir group compared with EVLP group (Fig. 2E, F). Thus, our results provide confirmation of the effectiveness of Lir perfusion in mitigating IRI in lung transplantation, showcasing its potential as a therapeutic strategy to improve transplant outcomes.

Lir down-regulates NOD-like receptors signal, and pyroptosis is present in lung transplant IRI

Although we have confirmed the attenuating effect of Lir perfusion on lung transplantation IRI, a comprehensive understanding of the underlying mechanism of Lir's action against IRI remains necessary. To this end, we employed tandem mass tag (TMT)-labeled quantitative proteomic analysis to evaluate global protein expression differences between the lung grafts of the EVLP group and EVLP + Lir group. This analysis identified 181 differentially expressed proteins (DEPs) meeting our criteria of a fold change ≥1.2 and a P-value < 0.05 (Fig. 3A), with 105 proteins significantly downregulated (the top 25 proteins are listed in Supplementary Table S1. http://links.lww.com/JS9/E136) and 76 upregulated in the EVLP + Lir group (the top 25 proteins are listed in Supplementary Table S2. http://links.lww.com/JS9/E136).

To elucidate the roles of these DEPs, we conducted a Gene Ontology (GO) functional enrichment analysis. Notably, the majority of the DEPs are involved in immune response modulation and cell death pathways, including I-kB kinase/NF-kB signaling, apoptotic signaling, and necroptotic signaling (Fig. 3B). These findings reinforce previous observations concerning the molecular-level repression of immune responses and cell death induced by Lir perfusion.

Additionally, we conducted a pathway analysis utilizing the KEGG database. Intriguingly, apart from the pathways related to inflammation, apoptosis, and necrosis, we observed a significant enrichment of the NOD -like receptors (NLRs) signaling pathway (Fig. 3C). Furthermore, a majority of component molecules within the NLRs signaling pathway exhibited downregulation in lung grafts subjected to Lir perfusion (Fig. 3D). Quantitative PCR (qPCR) analysis of lysates obtained from the lung grafts further confirmed a significant reduction in the gene expression of essential molecules involved in the NLRs signaling pathway (Fig. 3E).

Previous studies have demonstrated a strong correlation between the NLRs signaling pathway and the occurrence of

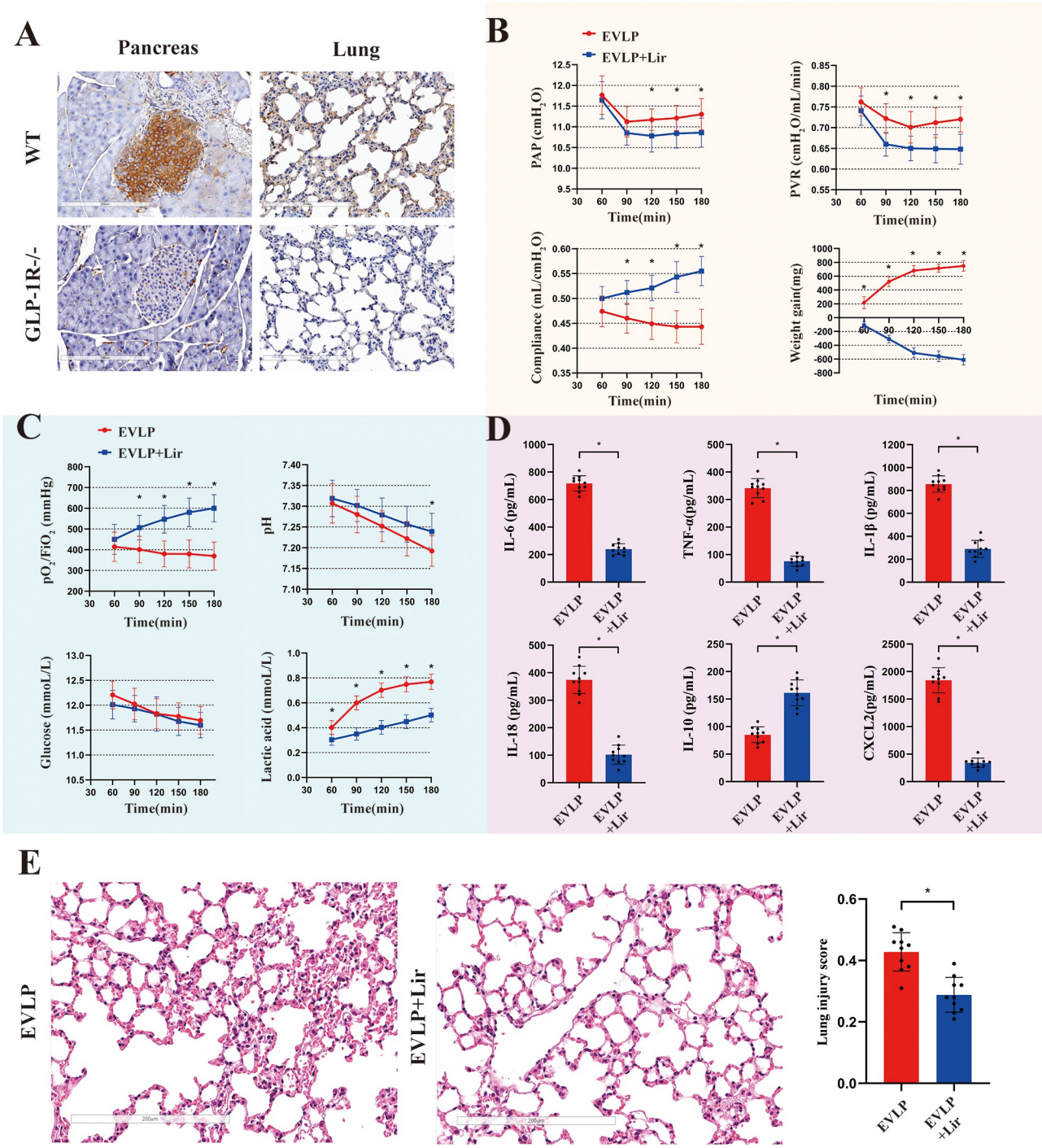

Figure 1. Lir improves DCD lung function and repairs injury during EVLP. (A) Representative images of GLP-1R immune-stained lung tissue and pancreatic islets in GLP-1R-/- mice and wild-type mice. During EVLP, (B) physiological parameters of perfusion, (C) oxygenation index (mmHg), pH, glucose (mmol/L), and lactic acid contents (mmoL/L), and (D) cytokine expression (pg/mL) of perfusate were compared between DCD lungs with Lir perfusion (100 nM) and with the control agent. (E) Representative images of H&E-stained lung tissue and the lung injury scores were compared between the DCD lungs of Lir and control agent perfusion. n =10 for the control group. n =10 for the EVLP LTx group. Two-tailed unpaired Student's t was used for B–E. *, Significant difference, $P < 0.05$. PAP, pulmonary artery pressure (cmH_2O). PVR, pulmonary vascular resistance (cmH_2O/mL/min). Compliance, lung compliance (mL/cmH_2O). Weight gain showed as mg.

pyroptosis[16,37-39]. Based on these findings, it can be inferred that pyroptosis is present in the context of lung transplant IRI. To substantiate this hypothesis, we assessed the presence of pyroptosis markers, namely IL-1β, IL-18, and NLRP3, in lung grafts from both the CI LTx and WI LTx groups (Supplementary Figure S4A. http://links.lww.com/JS9/E136). The activity of Caspase-1, which serves as the initiator of pyroptosis, was assessed in the aforementioned groups (Supplementary Figure

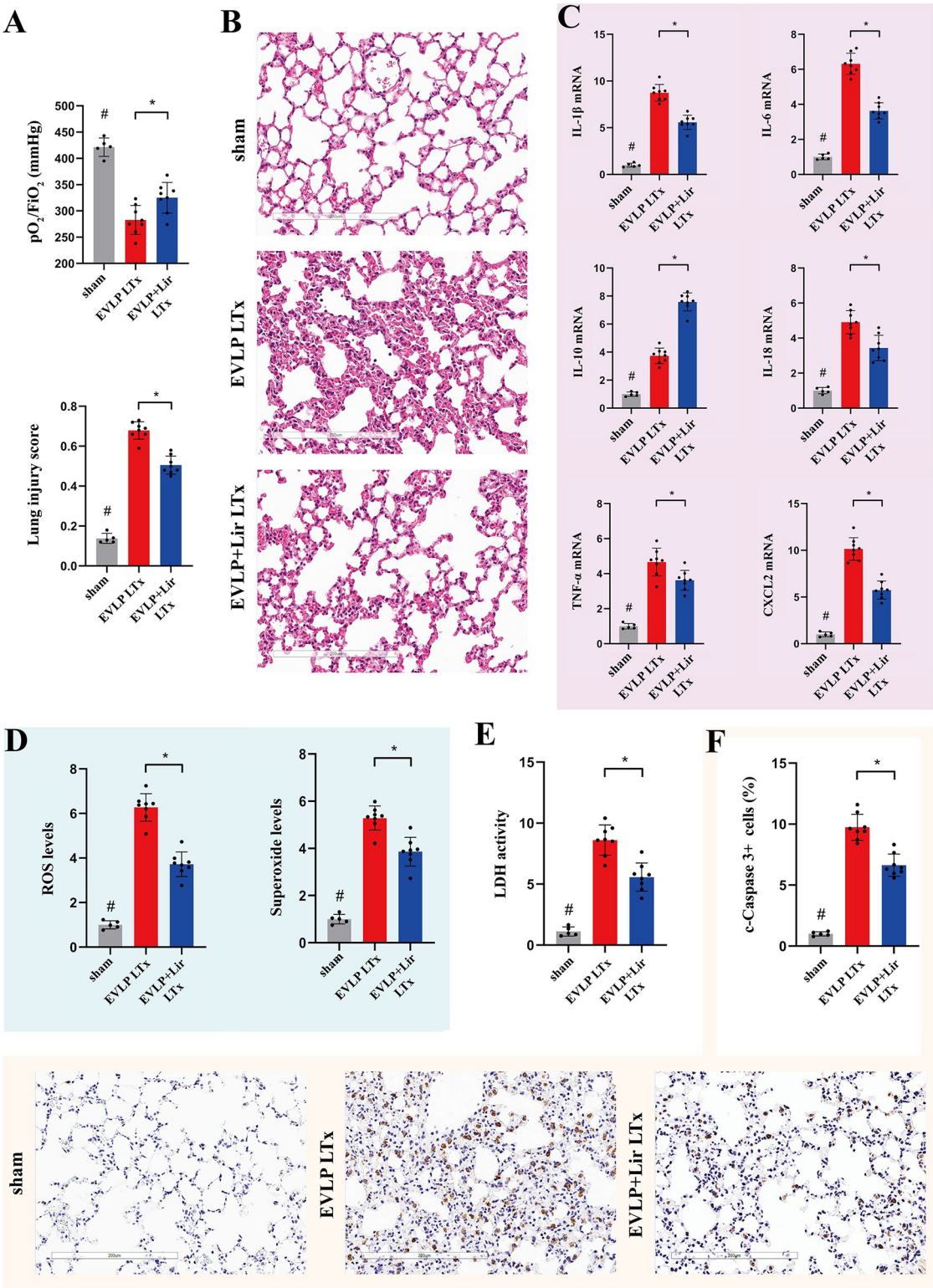

Figure 2. Lir perfusion by EVLP protects against IRI in lung transplantation. (A) Comparison of oxygenation indexes (mmHg) among the sham, EVLP, and EVLP + Lir groups of recipient rats. (B) Representative images of H&E-stained lung grafts and the lung injury score were compared among the three groups. (C) Cytokine and chemokine expression of lung grafts were compared among the three groups by q-PCR. The results were normalized to the β-actin levels. (D, E) The ROS and superoxide levels and LDH activity were compared among the three groups. These results are shown as relative units. (F) Representative images of cleaved-Caspase-3(immunohistochemistry stains nuclei) immune-stained lung grafts and quantification of cleaved-Caspase-3 positive cells were compared among the three groups. n =5 for the sham group. n =8 for the EVLP LTx group. n =8 for EVLP + Lir LTx group. One-way ANOVA was used for A–F. *, Significant difference, $P < 0.05$. #, significant difference, $P < 0.05$ compared with the EVLP LTx group or EVLP + Lir LTx group. qPCR, quantitative real-time polymerase chain reaction.

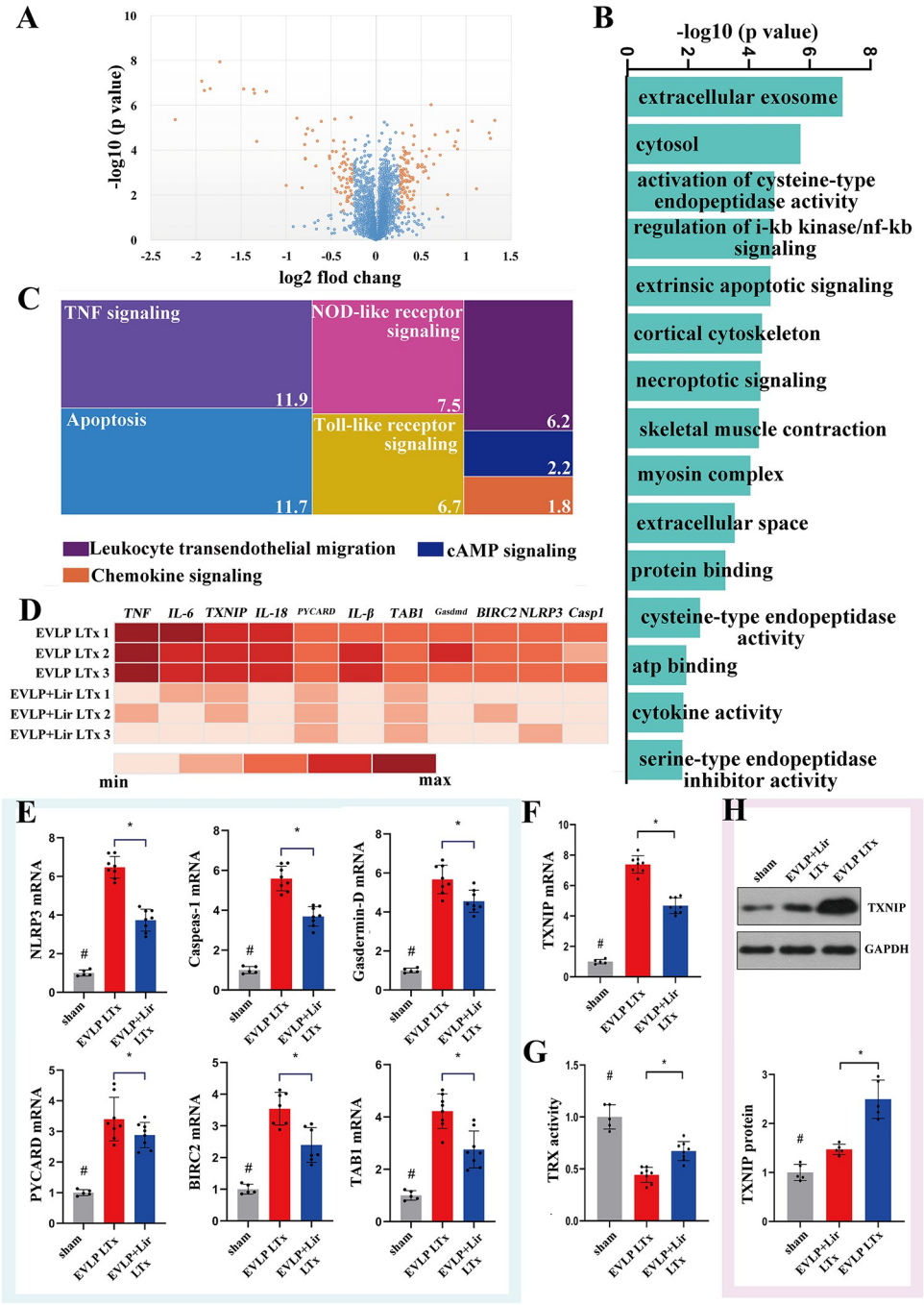

Figure 3. Lir down-regulates NOD-like receptors signal, TXNIP expression and function in lung grafts of DCD lung transplantation. TMT-labeled quantitative proteomic analysis was performed for global protein expression assay in the lung grafts of the EVLP group and EVLP + Lir group. (A) The volcanic map showed the distribution of DEPs in the lung grafts of the EVLP group and EVLP + Lir group. The DEPs were defined as fold change≥1.2 and $P < 0.05$ significance. (B) GO functional enrichment analysis for DEPs. (C) KEGG in DEPs pathway analysis. (D) The comparison of component molecule expression in the NLRs signaling pathway in lung grafts of the EVLP group and EVLP + Lir group. n =3 for per group. Lir perfusion by EVLP affects the expression of critical molecules of NLRs signaling pathway in lung grafts. (E)The mRNA expression of NLRP3, Caspeas-1, Gasdermin-D, PYCARD, BIRC2, and TAB1 was measured by qPCR in lung grafts of the sham, EVLP, and EVLP + Lir groups. (F) Comparison of TXNIP mRNA among the sham, EVLP LTx, and EVLP + Lir LTx groups of lung grafts by q-PCR test. The results were normalized to the β-actin levels. (G) Comparison of TRX activity among the three groups by using the insulin disulfide reduction assay. The results are shown as relative units. (H) Representative images of western blot analysis for TXNIP in lung grafts and the quantitative expression were compared among the three groups. The results were normalized to the GAPDH. n =5 for the sham group. n =8 for EVLP LTx group (n =5 for western blot analysis). n =8 for EVLP + Lir LTx group (n =5 for western blot analysis). One-way ANOVA was used for E–H. *, Significant difference, $P < 0.05$. #, significant difference, $P < 0.05$ compared with the EVLP LTx group or EVLP + Lir LTx group. NOD, nucleotide-binding and oligomerization domain. NLRs, NOD-like receptors. TMT, tandem mass tag. DEPs, differentially expressed proteins. GO, Gene Ontology. KEGG, Kyoto Encyclopedia of Genes and Genomes. PYCARD, PYD, and CARD domain-containing protein. BIRC2, baculoviral IAP repeat containing 2. TAB1, TGF-β activated kinase 1 (MAP3K7) binding protein 1. TRX, thioredoxin. GAPDH, glyceraldehyde-3-phosphate dehydrogenase.

S4B. http://links.lww.com/JS9/E136). Notably, the mRNA levels of IL-1β, IL-18, and NLRP3 as well as Caspase-1 activity, exhibited a significant increase in the WI LTx group compared to the sham and CI LTx groups. These findings collectively confirm the presence of pyroptosis in lung transplant IRI and suggest that Lir treatment may down-regulate pyroptosis.

TXNIP plays a critical role in pyroptosis in H/R-induced BEAS-2B cells and lung transplant IRI

The precise intracellular signaling mechanism that triggers pyroptosis in lung transplant IRI still remains poorly understood. In macrophages, oxidative stress triggered PAMPs or DAMPs is recognized as a crucial stimulus for pyroptosis[15,40-42]. To investigate this phenomenon, we employed MnTMPyP, a ROS scavenger, in BEAS-2B cells during H/R induction. While MnTMPyP effectively reduced ROS and superoxide levels (Fig. 6A), it did not alleviate the levels of IL-1β and Caspase-1 activity (Fig. 6B, C), suggesting that additional factors beyond ROS that could contribute to the pyroptosis activation in lung transplant IRI.

Further insight into these mechanisms was gained from our previous findings, which demonstrated that GLP-1RA ameliorated LPS-induced acute lung injury in mice by suppressing the TXNIP pathway[5]. In this study, the involvement of TXNIP in NLRs signal regulation by Lir was observed through proteomic analysis (Fig. 3D). Subsequent investigations revealed a significant downregulation of TXNIP mRNA and protein expression in the lung grafts of the EVLP + Lir group compared to the EVLP group (Fig. 3F, H). It was found that TXNIP binding inhibited TRX activity, reflecting TXNIP's functional role. Functional analysis further demonstrated that lung grafts from the EVLP + Lir group exhibited decreased TXNIP activity (Fig. 3G), underscoring the therapeutic potential of Lir in attenuating pyroptosis through modulation of the TXNIP pathway.

To investigate the impact of TXNIP on pyroptosis in non-immune cells, we employed recombinant adenoviruses (rAd-Null or rAd-TXNIP) to manipulate TXNIP expression in BEAS-2B cells. Following H/R induction, rAd-TXNIP-infected cells exhibited increased TXNIP expression and reduced cell viability (Supplementary Figure S5A, B. http://links.lww.com/JS9/E136). Compared to wild-type BEAS-2B cells, those overexpressing TXNIP displayed elevated levels of ROS and superoxideunder both standard and H/R conditions (Supplementary Figure S5C. http://links.lww.com/JS9/E136), as well as increased cell death, LDH activity and higher levels of IL-1β and IL-18 (Supplementary Figure S5D-F. http://links.lww.com/JS9/E136).

To further elucidate TXNIP's contribution to pyroptosis mediated by Lir, recombinant adeno-associated viruses (rAAV5-shTXNIP and rAAV5-TXNIP) were utilized to knock down (KD) or overexpress (OE) TXNIP in the lungs of donors undergoing EVLP followed by transplantation (Fig. 4A). Transcriptome and protein analyses of TXNIP indicated that the TXNIP KD EVLP LTx and TXNIP OE EVLP LTx groups, treated with rAAV5-shTXNIP and rAAV5-TXNIP, respectively, post-EVLP, exhibited significantly altered TXNIP levels compared to the WT EVLP LTx group treated with rAAV5-Null (Fig. 4B, C). Importantly, Lir administration during EVLP did not significantly alter TXNIP expression or activity in the TXNIP KD lung grafts (Fig. 4B, C, D).

Pathological assessments indicated that the TXNIP KD lung grafts had significantly fewer IRI lesions than both the TXNIP OE and WT grafts (Fig. 4E). In comparison to the control and TXNIP OE groups, the lung tissues from the TXNIP KD groups, with or without Lir treatment, exhibited more intact alveolar structures and lower degrees of mononuclear cell infiltration, as well as reduced interstitial and intra-alveolar edema. This observation was further supported by blinded pathological scoring, which showed a notable decrease in lung injury grades in the TXNIP KD group (Fig. 4E). Quantitative analyses revealed a reduction in cleaved Caspase-1-positive cells in TXNIP KD grafts, contrasting with the increase observed in the TXNIP OE group (Fig. 4F). Compared to the wild-type lung grafts, Lir treatment resulted in a modest decrease in cleaved-Caspase-1 positive cells in TXNIP KD lung grafts (Fig. 4F). Additionally, a low expression of TXNIP was associated with decreased LDH activity, whereas Lir treatment did not significantly impact LDH activity in the TXNIP KD lung grafts (Fig. 4G).

In this study, we analyzed the expression levels of IL-1β and TXNIP in BALF samples obtained from patients who underwent lung transplantation or other thoracic surgeries (serving as the control group) 48 hours post-surgery (the study was approved by the Ethics Committee. Our analysis indicated a marked increase in both IL-1β and TXNIP expression in the BALF of lung transplant patients compared to controls (Supplementary Figure S6A, B. http://links.lww.com/JS9/E136). Importantly, a positive correlation was identified between IL-1β and TXNIP levels in the BALF of lung transplant patients (Supplementary Figure S6C.http://links.lww.com/JS9/E136). These results suggest that TXNIP plays a critical role in the pyroptosis associated with IRI in lung transplantation.

Lir suppresses pyroptosis by regulating TXNIP/NLRP3 pathway

The activation of the NLRP3 inflammasome is a crucial event in pyroptosis[15]. However, the regulatory characteristics of Lir on the NLRP3 inflammasome remain unclear. To address this, BEAS-2B cells were infected with recombinant adenoviruses: rAd-NLRP3 to overexpress NLRP3, or rAd-shTXNIP to knock down TXNIP, followed by a H/R challenge. Our results demonstrated that TXNIP knockdown led to decreased NLRP3 expression (Fig. 5A), highlighting a regulatory interaction between TXNIP and NLRP3. Conversely, overexpressing NLRP3 in BEAS-2B cells enhanced the TXNIP-mediated NLRP3 inflammasome activation, subsequently elevating Caspase-1 and Caspase-3 activities (Fig. 5B) and facilitating cell death (Fig. 5C). Although Lir significantly reduce TXNIP levels in BEAS-2B cells with NLRP3 overexpression during the H/R challenge, it did not further decrease the activities of Caspase-1 and Caspase-3 (Fig. 5B), nor did it prevent cell death (Fig. 5C). These findings suggest that the regulatory effect of Lir on pyroptosis, specifically through the TXNIP pathway, is dependent on NLRP3.

Lir modulates TXNIP mRNA stability through a GLP-1R/miR-17-dependent manner

While we investigated the role of TXNIP in pyroptosis during lung transplant IRI and confirmed that Lir regulates pyroptosis through the TXNIP/NLRP3 pathway, the precise mechanism by which Lir regulates TXNIP remains unclear. It is important to note that ROS are responsible for inducing the upregulation of TXNIP[30,43,44]. However, in this study, MnTMPyP was unable to further decrease TXNIP levels in wild-type BEAS-2B cells under H/R conditions (Fig. 6D). This finding suggests that Lir regulates

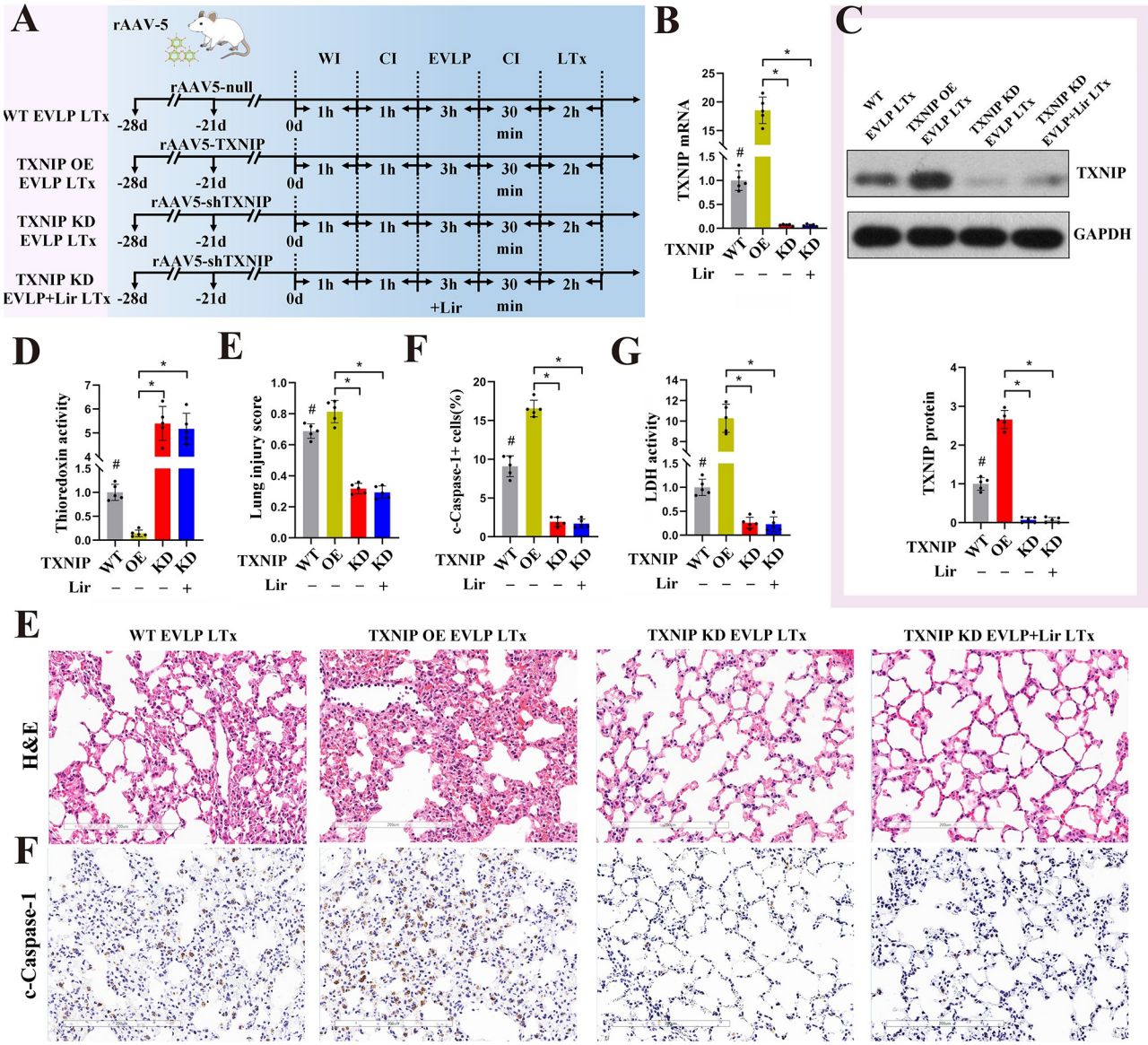

Figure 4. TXNIP plays a critical role in pyroptosis in lung transplant IRI. (A) Schematic diagram of the animal rAAV-5 infection experiment. (B, C) Compare TXNIP mRNA and protein expression among the WT EVLP LTx group, TXNIP OE EVLP LTx group, TXNIP KD EVLP LTx group, and TXNIP KD EVLP + Lir LTX group. (D and G) Comparison of TRX activity and LDH activity among the three groups. (E) Representative images of H&E-stained lung grafts and the lung injury scores were compared among the three groups. (F) Representative images of cleaved-Caspase-1(immunohistochemistry stains nuclei) immune-stained lung grafts, and quantification of cleaved-Caspase-1 positive cells were compared among the three groups. *n* =5 for per group, One-way ANOVA was used for B–E. *, Significant difference, $P < 0.05$. #, significant difference, $P < 0.05$ compared with the TXNIP OE EVLP LTx group, TXNIP KD EVLP LTx group, or TXNIP KD EVLP + Lir LTx group. rAAV, recombinant adeno-associated virus. WT, wild-type. OE, overexpression. KD, knock-down.

TXNIP in a ROS-independent manner. Further investigation revealed that Lir increased TXNIP ubiquitination in wild-type BEAS-2B cells under H/R conditions (Fig. 6E). Subsequently, we investigated the impact of GLP-1R knockdown on the effect of Lir on TXNIP ubiquitination under H/R conditions (Fig. 6E). Furthermore, we examined the effects of Lir on TXNIP modulation after proteasome inhibition by MG132 in BEAS-2B cells challenged with H/R. Compared to the control agent, pretreatment with MG132 did not diminish the impact of Lir on the regulation of TXNIP (Fig. 6F). These findings suggest that the GLP-1R-dependent ubiquitination pathway plays a role in the regulation of TXNIP by Lir. However, it is possible that the ubiquitin-proteasome system may not be the sole pathway through which GLP-1RA regulates TXNIP.

This study further explored the influence of Lir on TXNIP synthesis. Utilizing Actinomycin D to inhibit RNA synthesis in BEAS-2B cells revealed that TXNIP mRNA is typically unstable under normal culture conditions, progressively decreasing over time. However, under H/R conditions, TXNIP mRNA stability increased (Fig. 6G), suggesting a stress-related modulation of mRNA dynamics.

Through bioinformatics analysis using TargetScan (https://www.targetscan.org/vert_80/), we identified conserved micro RNA-17 (miR-17) binding sequences in the 3′ untranslated region

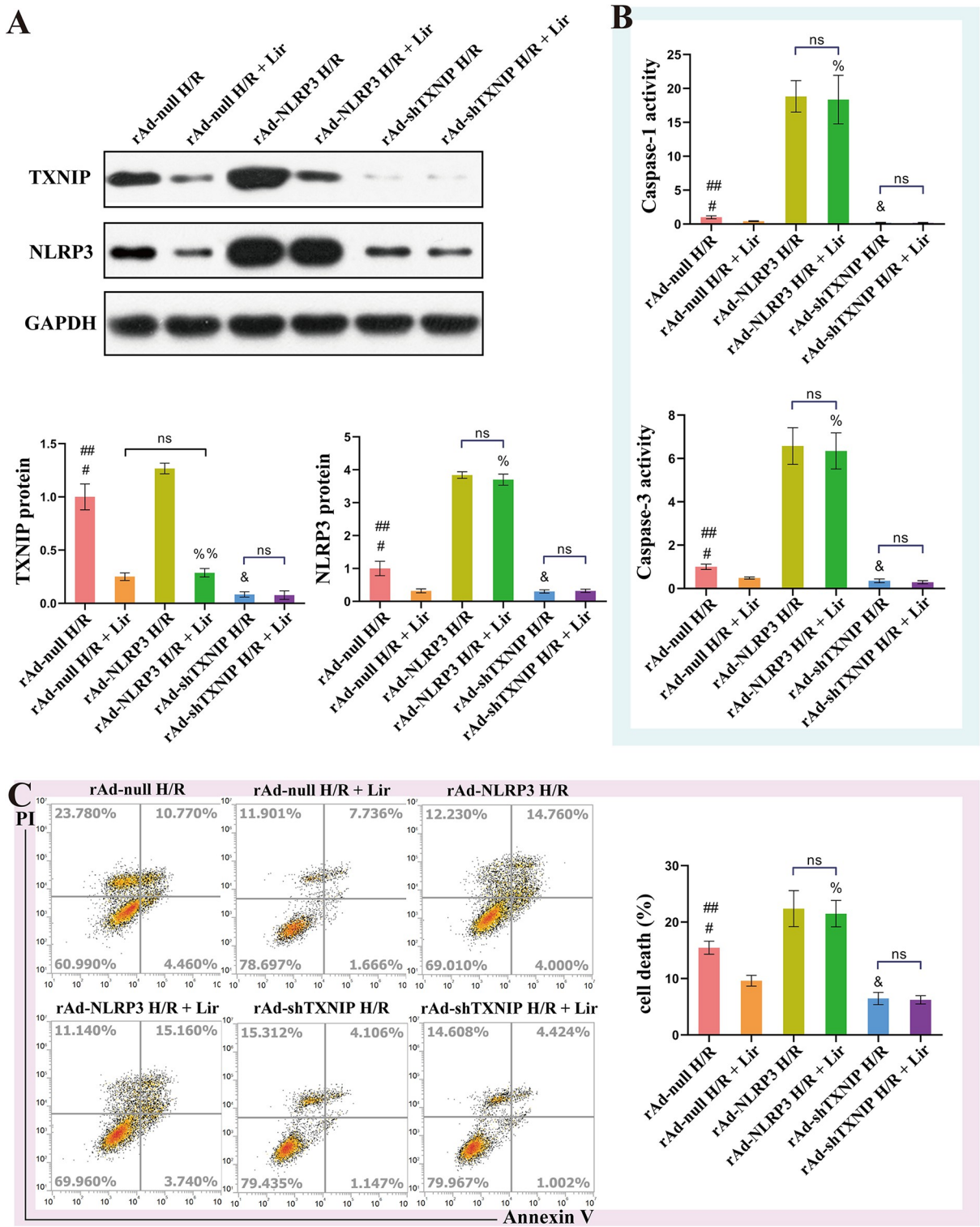

Figure 5. Lir suppresses pyroptosis by regulating the TXNIP/NLRP3 pathway. BEAS-2B cells were infected with recombinant adenovirus-null (rAd-null), rAd-NLRP3, or rAd-shTXNIP for 3 days, respectively. Later, BEAS-2B cells were treated with Lir (100 nM) or a control agent 24 hours before and during hypoxia/reoxygenation induction. (A) Representative images of western blot analysis for TXNIP and NLRP3 in BEAS-2B cells, and the quantitative expression were compared among the experimental groups. (B) Comparison of Caspase-1 and Caspase-3 activity by colorimetry. (C) Comparison of cell death by flow cytometry of Annexin V/PI staining (cell death defined as Annexin V +/PI +, Annexin V +/PI-). Data are representative of three independent experiments. Two-tailed unpaired Student's t was used for a–c. ns, Non-significant difference, $P > 0.05$. #, significant difference, $P < 0.05$ compared with the rAd-null H/R + Lir group. ##, significant difference, $P < 0.05$ compared with the rAd-NLRP3 H/R group. %, significant difference, $P < 0.05$ compared with the rAd-null H/R + Lir group. %%, significant difference, $P < 0.05$ compared with the rAd-NLRP3 H/R group. &, a significant difference, $P < 0.05$, compared with the rAd-null H/R group. rAd, recombinant adenovirus.PI, propidium iodide.

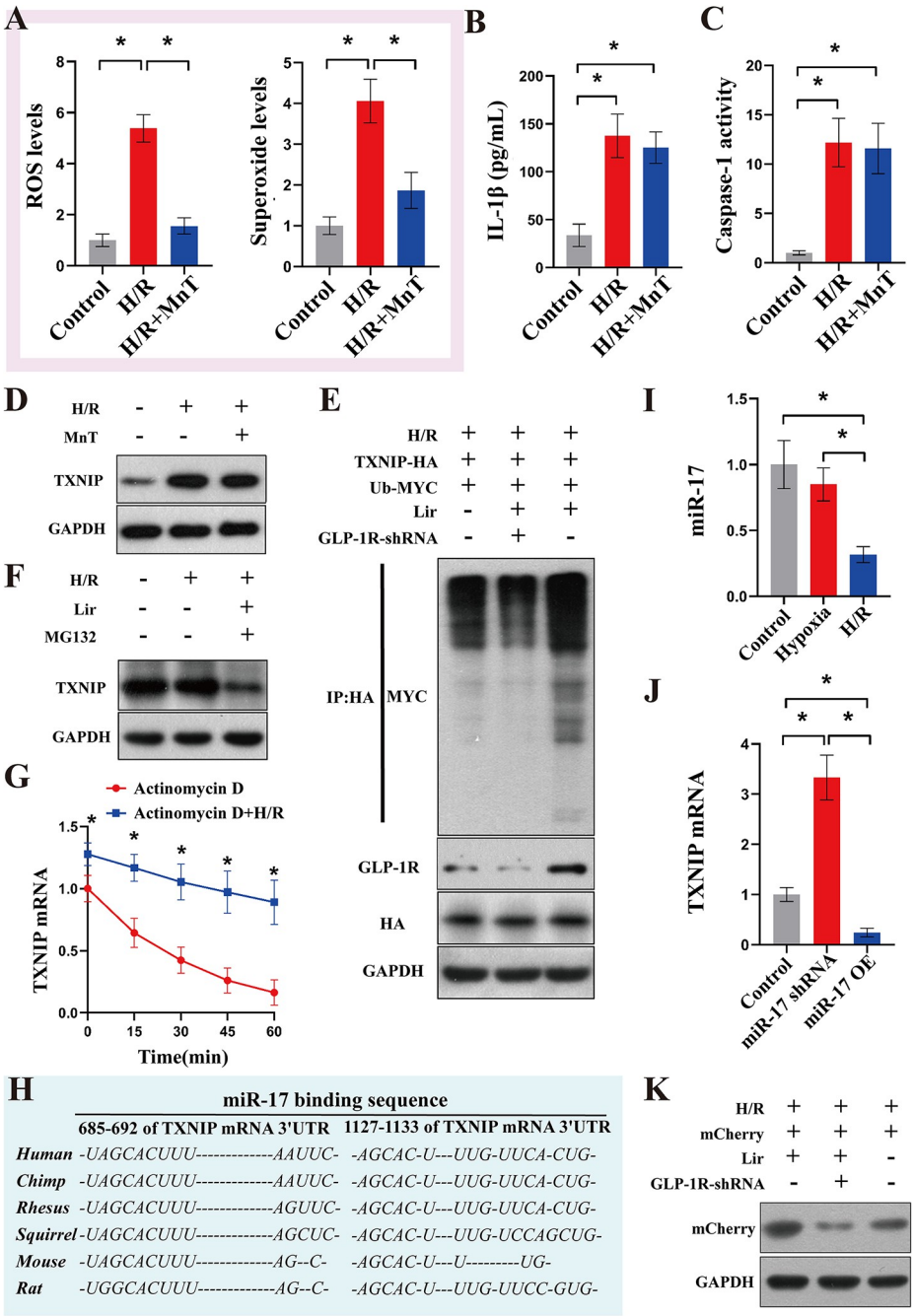

Figure 6. Lir enhances GLP-1R-dependent TXNIP ubiquitination, and modulates TXNIP mRNA stability in a GLP-1R/miR-17-dependent manner. MnTMPyP down-regulates oxidative stress but generates a weak reduction in pyroptosis and TXNIP expression in H/R-induced BEAS-2B cells.BEAS-2B cells were treated with a control agent or MnTMPyP (100 μM) 1 h before and during H/R induction (A) The ROS and superoxide levels were compared among the control, H/R, and H/R + MnT groups. These results showed as relative units. (B) The expression of IL-1β levels (pg/mL) were compared among the three groups by ELISA. (C) The Caspase-1 activity was compared among the three groups by colorimetry. The results showed as relative units. (D) TXNIP expression was detected by western blot. Lir enhances GLP-1R-dependent TXNIP ubiquitination, and modulates TXNIP mRNA stability in a GLP-1R/miR-17-dependent manner. BEAS-2B cells of wild-type or GLP-1R knock-down were treated with a control agent and Lir (100 nM) 24 h before and during H/R induction. (E) The cell lysates were subjected to immunoprecipitation (IP) for TXNIP, followed by western blotting for ubiquitin. (F) The wild-type BEAS-2B cells were pretreated with Lir (100 nM) or control agent for 24 h and MG132 (10 μM) or control agent for 1 h, followed by H/R induction. Western blot was used to detect TXNIP expression. (G) BEAS-2B cells were pretreated with Actinomycin D (5 mg/mL) for 4 h and treated with Actinomycin D (5 mg/mL) during hypoxia (3 h)/ reoxygenation (1 h) induction. The expression of TXNIP mRNA was detected by qPCR. (H) Multi-species conserved miR-17 binding sequence in TXNIP mRNA 3′untranslated region (red region). (I) miR-17 expression in BEAS-2B cells cultured in normal culture, hypoxia (3 h) or hypoxia (3 h)/reoxygenation (1 h) by q-PCR. (J) The TXNIP mRNA expression of BEAS-2B cells with miR-17 knock-down or overexpression in H/R condition. (K) The expression of mCherry (miR-17) in wild-type and GLP-1R knock-down BEAS-2B cells, which were treated with a control agent or Lir (100 nM) in H/R condition, was detected by western blot. Data are representative of three independent experiments. Two-tailed unpaired Student's t was used for g. One-way ANOVA was used for a, b, i and j. *, Significant difference, $P < 0.05$. Ub, ubiquitin. MG132, a proteasome inhibitor.

of TXNIP mRNA (Fig. 6H). Following H/R induction, a significant decrease in miR-17 expression was observed in BEAS-2B cells (Fig. 6I). Comparatively, in BEAS-2B cells subjected to H/R conditions, knockdown of miR-17 in BEAS-2B cells resulted in increased TXNIP mRNA expression, while overexpression of miR-17 led to decreased TXNIP mRNA levels (Fig. 6J).

Further investigation was conducted to determine whether Lir affects miR-17 regulation. BEAS-2B cells were transfected with a fluorescent reporter gene containing the miR-17 sequence, with the expression intensity of the red fluorescent protein served as an indicator of Lir's impact on endogenous miR-17 expression. The results indicated that Lir upregulated miR-17 expression. However, this effect was diminished when the GLP-1R was knocked down (Fig. 6K), suggesting that Lir's modulation of miR-17 is mediated through the GLP-1R pathway.

Consequently, H/R induction leads to an upregulation of miR-17 expression and affects the stability of TXNIP mRNA. Moreover, Lir may regulate miR-17 expression through the GLP-1R pathway.

Discussion

DCD and donation after brain death (DBD) are the main sources of donor lungs for transplantation, often considered marginal due to risks like infection, edema, injury, and prolonged warm ischemia,, which increase the risk of IRI and cell death[45-47]. This study emphasizes the role of pyroptosis in lung transplant IRI, adding to previous research focused on apoptosis and necrosis[2,13,47].

Prior studies on pyroptosis have mainly examined immune cells in infections and autoimmune diseases. Noda *et al* linked Caspase-1 expression to increased leukocyte pyroptosis in donor mice lungs, affecting graft quality[18]. Our study found that lung transplant IRI boosts pyroptosis markers such as IL-1β, IL-18, NLRP3, and mature Caspase-1 in lung grafts.

Further, we observed down-regulation of NLR signaling in lung grafts with Lir, indicating pyroptosis in lung transplant IRI. Previous studies showed Caspase-11-mediated pyroptosis in endothelial cells during lung injury, but research on non-immune cell pyroptosis in lung transplant IRI is limited[48]. However, Our findings highlight the role of non-immune cell pyroptosis, with increased IL-1β and IL-18 expression and cell death in BEAS-2B cells under H/R conditions. This suggests that interventions aimed at modulating pyroptosis could represent a novel and promising approach to improving lung graft viability and function post-transplant.

Modulating pyroptosis might improve lung graft viability post-transplant, as oxidative stress exacerbates lung transplant IRI[49-51]. Emerging evidence indicates that ROS are crucial for initiating pyroptosis[52-54]. However, our experiments show that merely reducing ROS levels does not significantly affect pyroptosis in H/R-induced BEAS-2B cells, highlighting a complex interaction with other mediators.

TXNIP, a key oxidative stress mediator and NLRP inflammasome component, is widely present in the body[55,56]. As a critical mediator of oxidative stress and a component of the NLRP inflammasome, TXNIP has been proposed as a potential therapeutic target for IRI and other disorders[57-59]. In the context of lung grafts, we noted a significant increase in TXNIP function and expression. Analyzing TXNIP-overexpressed BEAS-2B cells under H/R stimulus, we found that TXNIP directly increased ROS, superoxide, and the expression of IL-1β and IL-18.

Conversely, inhibiting TXNIP reduces NLRP3 expression and Caspase-1 activity. Overexpressing NLRP3 in BEAS-2B cells increases TXNIP during H/R induction. In the model of lung transplantation from DCD, TXNIP suppression decreases cleaved-Caspase-1. Notably, TXNIP and IL-1β levels are higher in BALF from lung transplant patients than controls. This study reveals that H/R or lung transplant IRI elevates TXNIP, linked to pyroptosis.

It also supports previous findings that Lir treatment reduces LPS-induced TXNIP and apoptosis via GLP-1R[5]. Other studies show GLP-1R activation affects NADPH oxidase through cAMP/PKA, lowering TXNIP by inhibiting ROS[60-62]. In addition, exenatide treatment has been shown to stimulate the up-regulation of TXNIP ubiquitination[63]. Our current findings extend this understanding by demonstrating that Lir boosts TXNIP ubiquitination even when the proteasome is inhibited by MG132.

It is well-established that miRNAs play a crucial role in regulating mRNA stability[64,65]. This study, for the first time, elucidates that Lir regulated TXNIP mRNA stability through the GLP-1R/miR-17 pathway. Given these findings and the absence of specific therapeutic agents for PGD, GLP-1-based drugs may offer distinct advantages as targeted therapy for lung transplant IRI.

Various therapeutic strategies are being integrated into EVLP management to enhance donor lung quality, both in laboratory and clinical setting[66-68]. These include drug infusion (adenosine agonists[69], alpha-anti-trypsin[12]), inhalation of therapeutic gases (NO, CO, H_2)[70-72], intrabronchial administration of pulmonary surfactant[71], IL-10 gene therapy[73], stem cell therapy[74], and high-dose antibiotics for the treatment of infections[75]. A recent study even demonstrated the potential of light therapies during EVLP to inactivate the hepatitis C virus in donor lungs[74]. In this study, we utilized EVLP as a drug delivery platform for Lir, demonstrating its efficacy in delivering the drug for lung reconditioning to mitigate lung transplant IRI. We propose that EVLP not only serves as an effective delivery system, reducing potential systemic side effects, but also as a novel, organ-specific drug screening platform. This unique approach allows for direct action on specific biological targets within the lung while avoiding the complexities and systemic reactions associated with *in vivo* drug screening.

Animal models inherently differ from humans in their immune responses, lung architecture, and systemic physiology, and in vitro models cannot fully replicate the dynamic complexity of the in vivo environment. However, these models provide essential mechanistic insights into the cellular and molecular changes that occur during IRI and the potential benefits of GLP-1R agonist treatment. In light of these model limitations, further validation in large animal models and human clinical trials will be necessary to confirm the therapeutic potential of GLP-1R agonists in lung transplantation.

Conclusion

In summary, this study demonstrates for the first time that using a novel EVLP-based drug delivery approach using GLP-1RA can protect lungs from IRI by modulating pyroptosis, thereby improving lung function and reducing injury. Importantly, the research uncovers a previously unknown mechanism in which GLP-1RAs modulates the protein TXNIP through GLP-1R/miR-17 signaling. These insights underscore the potential of GLP-1RAs as targeted therapies for PGD in lung transplant recipients, opening new

avenues for clinical interventions aimed at improving transplant outcomes.

Ethical approval

This study was reviewed and approved by the Ethical Committee of Shanghai Chest Hospital affiliated with Shanghai Jiao Tong University School of Medicine [approval number: KS(Y)21172].

Consent

Not applicable.

Sources of funding

The present study was supported in part by the National Natural Science Foundation of China (82170108, 81700092, 22304067), the Clinical Research Projects in Health industry of Shanghai Municipal Health Commission (202340017), the Foundation of the Center for Medical and Engineering Interdisciplinary Innovation, University of Shanghai for Science and Technology (2023GD-XK08Z), the Basic Research Foundation of Shanghai Chest Hospital (2020YNJCM05), and Shanghai Leading Talent Program of Eastern Talent Plan (CYQN2023031).

Author contributions

Y.Z.: Data curation; formal analysis; investigation; visualization; methodology; project administration; Writing – original draft. T.L.: Conceptualization; data curation; formal analysis; validation; methodology; writing-review and editing. H.G.: Data curation; formal analysis; validation; investigation; writing-review and editing. J.S.: Data curation; formal analysis; validation; visualization; methodology; J.Y.: Data curation; formal analysis; validation. S.F.: Data curation; formal analysis; validation. X.P.: Data curation; formal analysis; validation. F.L.: Data curation; formal analysis; validation; investigation. H.Z.: Data curation; formal analysis; validation. D.Z.: Formal analysis; investigation; methodology. H.Y., L. Z., M.S.: Conceptualization; resources; supervision; project administration; writing-review and editing. W.Z: Conceptualization; funding acquisition; resources; supervision; formal analysis; writing-original draft; project administration; writing-review and editing.

Conflicts of interest disclosure

The authors declare that they have no competing interests.

Research registration unique identifying number (UIN)

Not applicable.

Guarantor

Wenyong Zhou

Provenance and peer review

Not commissioned, externally peer-reviewed.

Data availability statement

Not applicable.

References

[1] Kulkarni HS, Ramphal K, Ma L, *et al*. Local complement activation is associated with primary graft dysfunction after lung transplantation. JCI Insight 2020;5:e138358.
[2] Wang X, O'Brien ME, Yu J, *et al*. Prolonged cold ischemia induces necroptotic cell death in ischemia-reperfusion injury and contributes to primary graft dysfunction after lung transplantation. Am J Respir Cell Mol Biol 2019;61:244–56.
[3] Zhou W, Yang J, Saren G, *et al*. HDAC6-specific inhibitor suppresses Th17 cell function via the HIF-1α pathway in acute lung allograft rejection in mice. Theranostics 2020;10:6790–805.
[4] Muskiet MHA, Tonneijck L, Smits MM, *et al*. GLP-1 and the kidney: from physiology to pharmacology and outcomes in diabetes. Nat Rev Nephrol 2017;13:605–28.
[5] Zhou W, Shao W, Zhang Y, Liu D, Liu M, Jin T. Glucagon-like peptide-1 receptor mediates the beneficial effect of liraglutide in an acute lung injury mouse model involving the thioredoxin-interacting protein. Am J Physiol Endocrinol Metab 2020;319:E568–E578.
[6] Wiberg S, Hassager C, Schmidt H, *et al*. Neuroprotective effects of the glucagon-like peptide-1 analog exenatide after out-of-hospital cardiac arrest: a randomized controlled trial. Circulation 2016;134:2115–24.
[7] Prattichizzo F, de Candia P, Ceriello A. Diabetes and kidney disease: emphasis on treatment with SGLT-2 inhibitors and GLP-1 receptor agonists. Metabolism 2021;120:154799.
[8] Motoyama H, Chen F, Hijiya K, *et al*. Plasmin administration during ex vivo lung perfusion ameliorates lung ischemia-reperfusion injury. J Heart Lung Transplant 2014;33:1093–99.
[9] Tane S, Noda K, Shigemura N. Ex vivo lung perfusion: a key tool for translational science in the lungs. Chest 2017;151:1220–28.
[10] Wang A, Ali A, Keshavjee S, Liu M, Cypel M. Ex vivo lung perfusion for donor lung assessment and repair: a review of translational interspecies models. Am J Physiol Lung Cell Mol Physiol 2020;319:L932–L940.
[11] Galasso M, Feld JJ, Watanabe Y, *et al*. Inactivating hepatitis C virus in donor lungs using light therapies during normothermic ex vivo lung perfusion. Nat Commun 2019;10:481.
[12] Lin H, Chen M, Tian F, *et al*. α1-Anti-trypsin improves function of porcine donor lungs during ex-vivo lung perfusion. J Heart Lung Transplant 2018;37:656–66.
[13] Kanou T, Ohsumi A, Kim H, *et al*. Inhibition of regulated necrosis attenuates receptor-interacting protein kinase 1-mediated ischemia-reperfusion injury after lung transplantation. J Heart Lung Transplant 2018;37:1261–70.
[14] Fischer S, Maclean AA, Liu M, *et al*. Dynamic changes in apoptotic and necrotic cell death correlate with severity of ischemia-reperfusion injury in lung transplantation. Am J Respir Crit Care Med 2000;162:1932–39.
[15] Broz P, Dixit VM. Inflammasomes: mechanism of assembly, regulation and signalling. Nat Rev Immunol 2016;16:407–20.
[16] Xue Y, Enosi Tuipulotu D, Tan WH, Kay C, Man SM. Emerging activators and regulators of inflammasomes and pyroptosis. Trends Immunol 2019;40:1035–52.
[17] Rathinam VAK, Fitzgerald KA. Inflammasome complexes: emerging mechanisms and effector functions. Cell 2016;165:792–800.
[18] Noda K, Tane S, Haam SJ, *et al*. Targeting circulating leukocytes and pyroptosis during ex vivo lung perfusion improves lung preservation. Transplantation 2017;101:2841–49.
[19] Abderrazak A, Syrovets T, Couchie D, *et al*. NLRP3 inflammasome: from a danger signal sensor to a regulatory node of oxidative stress and inflammatory diseases. Redox Biol 2015;4:296–307.
[20] Watanabe R, Nakamura H, Masutani H, Yodoi J. Anti-oxidative, anti-cancer and anti-inflammatory actions by thioredoxin 1 and thioredoxin-binding protein-2. Pharmacol Ther 2010;127:261–70.
[21] Saxena G, Chen J, Shalev A. Intracellular shuttling and mitochondrial function of thioredoxin-interacting protein. J Biol Chem 2010;285:3997–4005.
[22] Kilkenny C, Browne WJ, Cuthill IC, Emerson M, Altman DG. Improving bioscience research reporting: the ARRIVE guidelines for reporting animal research. PLoS Biol 2010;8:e1000412.
[23] Wang X, Parapanov R, Debonneville A, *et al*. Treatment with 3-aminobenzamide during ex vivo lung perfusion of damaged rat lungs

reduces graft injury and dysfunction after transplantation. Am J Transplant 2020;20:967–76.
[24] Goto T, Kohno M, Anraku M, Ohtsuka T, Izumi Y, Nomori H. Simplified rat lung transplantation using a new cuff technique. Ann Thorac Surg 2012;93:2078–80.
[25] Zhou W, Shao W, Zhang Y, Liu D, Liu M, Jin T. Glucagon-like peptide-1 receptor mediates the beneficial effect of liraglutide in an acute lung injury mouse model involving the thioredoxin-interacting protein. Am J Physiol Endocrinol Metab 2020;319:E568–e578.
[26] Matute-Bello G, Downey G, Moore BB, *et al*. An official American thoracic society workshop report: features and measurements of experimental acute lung injury in animals. Am J Respir Cell Mol Biol 2011;44:725–38.
[27] Jensen CB, Pyke C, Rasch MG, Dahl AB, Knudsen LB, Secher A. Characterization of the glucagonlike peptide-1 receptor in male mouse brain using a novel antibody and in situ hybridization. Endocrinology 2018;159:665–75.
[28] Del Bino G, Darzynkiewicz Z, Degraef C, Mosselmans R, Fokan D, Galand P. Comparison of methods based on annexin-V binding, DNA content or TUNEL for evaluating cell death in HL-60 and adherent MCF-7 cells. Cell Prolif 1999;32:25–37.
[29] Tao L, Gao E, Jiao X, *et al*. Adiponectin cardioprotection after myocardial ischemia/reperfusion involves the reduction of oxidative/nitrative stress. Circulation 2007;115:1408–16.
[30] Gao C, Wang R, Li B, *et al*. TXNIP/Redd1 signalling and excessive autophagy: a novel mechanism of myocardial ischaemia/reperfusion injury in mice. Cardiovasc Res 2020;116:645–57.
[31] Tonack S, Aspinall-O'Dea M, Jenkins RE, *et al*. A technically detailed and pragmatic protocol for quantitative serum proteomics using iTRAQ. J Proteomics 2009;73:352–56.
[32] Yin J, You S, Li N., *et al*. Lung-specific RNA interference of coupling factor 6, a novel peptide, attenuates pulmonary arterial hypertension in rats. Respir Res 2016;17:99.
[33] Meja KK, Catley MC, Cambridge LM, *et al*. Adenovirus-mediated delivery and expression of a cAMP-dependent protein kinase inhibitor gene to BEAS-2B epithelial cells abolishes the anti-inflammatory effects of rolipram, salbutamol, and prostaglandin E2: a comparison with H-89. J Pharmacol Exp Ther 2004;309:833–44.
[34] Mikami M, Perez-Zoghbi JF, Zhang Y, Emala CW. Attenuation of murine and human airway contraction by a peptide fragment of the cytoskeleton regulatory protein gelsolin. Am J Physiol Lung Cell Mol Physiol 2019;316:L105–L113.
[35] Sharma AK, Charles EJ, Zhao Y, *et al*. Pannexin-1 channels on endothelial cells mediate vascular inflammation during lung ischemia-reperfusion injury. Am J Physiol Lung Cell Mol Physiol 2018;315:L301–L312.
[36] Pang J, Feng JN, Ling W, Jin T. The anti-inflammatory feature of glucagon-like peptide-1 and its based diabetes drugs-therapeutic potential exploration in lung injury. Acta Pharm Sin B 2022;12:4040–55.
[37] Burdette BE, Esparza AN, Zhu H, Wang S. Gasdermin D in pyroptosis. Acta Pharm Sin B 2021;11:2768–82.
[38] Swanson KV, Deng M, Ting JPY. The NLRP3 inflammasome: molecular activation and regulation to therapeutics. Nat Rev Immunol 2019; 19:477–89.
[39] Gaul S, Leszczynska A, Alegre F, *et al*. Hepatocyte pyroptosis and release of inflammasome particles induce stellate cell activation and liver fibrosis. J Hepatol 2021;74:156–67.
[40] Robinson N, Ganesan R, Hegedűs C, Kovács K, Kufer TA, Virág L. Programmed necrotic cell death of macrophages: focus on pyroptosis, necroptosis, and parthanatos. Redox Biol 2019;26:101239.
[41] Wang Y, Shi P, Chen Q, *et al*. Mitochondrial ROS promote macrophage pyroptosis by inducing GSDMD oxidation. J Mol Cell Biol 2019;11: 1069–82.
[42] Fidler TP, Xue C, Yalcinkaya M, *et al*. The AIM2 inflammasome exacerbates atherosclerosis in clonal haematopoiesis. Nature 2021;592:296–301.
[43] Han Y, Xu X, Tang C, *et al*. Reactive oxygen species promote tubular injury in diabetic nephropathy: the role of the mitochondrial ros-txnip-nlrp3 biological axis. Redox Biol 2018;16:32–46.
[44] Lv H, Zhu C, Wei W, *et al*. Enhanced keap1-nrf2/trx-1 axis by daphnetin protects against oxidative stress-driven hepatotoxicity via inhibiting ASK1/JNK and txnip/NLRP3 inflammasome activation. Phytomedicine 2020;71:153241.
[45] Avtaar Singh SS, Banner NR, Rushton S, Simon AR, Berry C, Al-Attar N. ISHLT primary graft dysfunction incidence, risk factors, and outcome: a UK national study. Transplantation 2019;103:336–43.
[46] Lardinois D, Banysch M, Korom S, *et al*. Extended donor lungs: eleven years experience in a consecutive series. Eur J Cardiothorac Surg 2005;27:762–67.
[47] Thabut G, Mal H, Cerrina J, *et al*. Graft ischemic time and outcome of lung transplantation: a multicenter analysis. Am J Respir Crit Care Med 2005;171:786–91.
[48] Cheng KT, Xiong S, Ye Z, *et al*. Caspase-11-mediated endothelial pyroptosis underlies endotoxemia-induced lung injury. J Clin Invest 2017;127:4124–35.
[49] Kim J-L, Reader BF, Dumond C, *et al*. Pegylated-catalase is protective in lung ischemic injury and oxidative stress. Ann Thorac Surg 2021;111:1019–27.
[50] Reid D, Snell G, Ward C, *et al*. Iron overload and nitric oxide-derived oxidative stress following lung transplantation. J Heart Lung Transplant 2001;20:840–49.
[51] Kozower BD, Christofidou-Solomidou M, Sweitzer TD, *et al*. Immunotargeting of catalase to the pulmonary endothelium alleviates oxidative stress and reduces acute lung transplantation injury. Nat Biotechnol 2003;21:392–98.
[52] Evavold CL, Hafner-Bratkovič I, Devant P, *et al*. Control of gasdermin D oligomerization and pyroptosis by the ragulator-rag-mTORC1 pathway. Cell 2021;184:4495-511.
[53] Li M-Y, Zhu X-L, Zhao B-X, *et al*. Adrenomedullin alleviates the pyroptosis of Leydig cells by promoting autophagy via the ROS-AMPK-mTOR axis. Cell Death Dis 2019;10:489.
[54] Zhang C, Lin T, Nie G, *et al*. Cadmium and molybdenum co-induce pyroptosis via ROS/PTEN/PI3K/AKT axis in duck renal tubular epithelial cells. Environ Pollut 2021;272:116403.
[55] Dai X, Liao R, Liu C, *et al*. Epigenetic regulation of TXNIP-mediated oxidative stress and NLRP3 inflammasome activation contributes to SAHH inhibition-aggravated diabetic nephropathy. Redox Biol 2021;45:102033.
[56] Tsubaki H, Tooyama I, Walker DG. Thioredoxin-interacting protein (TXNIP) with focus on brain and neurodegenerative diseases. Int J Mol Sci 2020; 21:9357.
[57] Cheng S-B, Nakashima A, Huber WJ, *et al*. Pyroptosis is a critical inflammatory pathway in the placenta from early onset preeclampsia and in human trophoblasts exposed to hypoxia and endoplasmic reticulum stressors. Cell Death Dis 2019;10:927.
[58] Jun JH, Shim J-K, Oh JE, Shin E-J, Shin E, Kwak Y-L. Protective effect of ethyl pyruvate against myocardial ischemia reperfusion injury through regulations of ros-related nlrp3 inflammasome activation. Oxid Med Cell Longev 2019;2019:4264580.
[59] Lv Z, Wang Y, Liu Y-J, *et al*. NLRP3 inflammasome activation contributes to mechanical stretch-induced endothelial-mesenchymal transition and pulmonary fibrosis. Crit Care Med 2018;46:e49–e58.
[60] Li N, Li B, Brun T, *et al*. NADPH oxidase NOX2 defines a new antagonistic role for reactive oxygen species and cAMP/PKA in the regulation of insulin secretion. Diabetes 2012;61:2842–50.
[61] Zhao L, Li AQ, Zhou TF, Zhang MQ, Qin XM. Exendin-4 alleviates angiotensin II-induced senescence in vascular smooth muscle cells by inhibiting rac1 activation via a cAMP/PKA-dependent pathway. Am J Physiol Cell Physiol 2014;307:C1130–C1141.
[62] Fujita H, Morii T, Fujishima H, *et al*. The protective roles of GLP-1R signaling in diabetic nephropathy: possible mechanism and therapeutic potential. Kidney Int 2014;85:579–89.
[63] Shao W, Yu Z, Fantus IG, Jin T. Cyclic AMP signaling stimulates proteasome degradation of thioredoxin interacting protein (txNIP) in pancreatic beta-cells. Cell Signal 2010;22:1240–46.
[64] Fabian MR, Sonenberg N, Filipowicz W. Regulation of mRNA translation and stability by microRNAs. Annu Rev Biochem 2010;79:351–79.
[65] Zhu K-P, Zhang C-L, Ma X-L, Hu J-P, Cai T, Zhang L. Analyzing the Interactions of mRNAs and ncRNAs to predict competing endogenous rna networks in osteosarcoma chemo-resistance. Mol Ther 2019;27: 518–30.
[66] Okamoto T, Ayyat KS, Sakanoue I, *et al*. Clinical significance of donor lung weight at procurement and during ex vivo lung perfusion. J Heart Lung Transplant 2022;41:818–28.
[67] Li SS, Funamoto M, Singh R, *et al*. Outcomes of donation after circulatory death (DCD) and ex-vivo lung perfusion (EVLP) lung transplantation. J Heart Lung Transplant 2024;44:721-33.
[68] Divithotawela C, Cypel M, Martinu T., *et al*. Long-term outcomes of lung transplant with ex vivo lung perfusion. JAMA Surg 2019;154: 1143–50.

[69] Stone ML, Sharma AK, Mas VR, *et al*. Ex vivo perfusion with adenosine a2a receptor agonist enhances rehabilitation of murine donor lungs after circulatory death. Transplantation 2015;99:2494–503.
[70] Noda K, Shigemura N, Tanaka Y, *et al*. Hydrogen preconditioning during ex vivo lung perfusion improves the quality of lung grafts in rats. Transplantation 2014;98:499–506.
[71] Dong B, Stewart PW, Egan TM. Postmortem and ex vivo carbon monoxide ventilation reduces injury in rat lungs transplanted from non-heart-beating donors. J Thorac Cardiovasc Surg 2013;146:429-36.
[72] Tavasoli F, Liu M, Machuca T, *et al*. Increased arginase expression and decreased nitric oxide in pig donor lungs after normothermic ex vivo lung perfusion. Biomolecules 2020;10:300.
[73] Yeung JC, Wagnetz D, Cypel M, *et al*. Ex vivo adenoviral vector gene delivery results in decreased vector-associated inflammation pre- and post-lung transplantation in the pig. Mol Ther 2012;20: 1204–11.
[74] Lonati C, Bassani GA, Brambilla D, *et al*. Mesenchymal stem cell-derived extracellular vesicles improve the molecular phenotype of isolated rat lungs during ischemia/reperfusion injury. J Heart Lung Transplant 2019;38:1306–16.
[75] Andreasson A, Karamanou DM, Perry JD, *et al*. The effect of ex vivo lung perfusion on microbial load in human donor lungs. J Heart Lung Transplant 2014;33:910–16.